RP Current Trends in Engineering and Technology
Vol. 1, No. 2 (August 2022) pp. 38–42
e-ISSN: 2583-5491

Cite this article: M. Kumari, A comparative study of acoustical phonon induced and optical phonon induced parametric gain in $A^{III}B^{V}$ semiconductor-magneto-plasmas, *RP Cur. Tr. Eng. Tech.* **1** (2022) 38–42.

Original Research Article

A comparative study of acoustical phonon induced and optical phonon induced parametric gain in $A^{III}B^{V}$ type semiconductor-magneto-plasmas

Manju Kumari
Department of Physics, Government College, Birohar – 124106, Jhajjar, Haryana, India
*Corresponding author, E-mail: manjudalal.sk@gmail.com

ARTICLE HISTORY
Received: 22 June 2022
Revised: 19 August 2022
Accepted: 21 August 2022
Published online:
24 August 2022

KEYWORDS
Parametric gain;
acoustical phonon;
optical phonon;
$A^{III}B^{V}$ type semiconductor-plasmas; threshold;
gain coefficient.

ABSTRACT
The purpose of this research is to compare and contrast the parametric amplification caused by acoustical phonons and optical phonons in magnetised doped III-V semiconductors. The threshold pump amplitude for the onset of optical and acoustic phonon-driven instability, as well as the related gain coefficients well above the threshold field, have been explicitly expressed using a hydrodynamic model of a semiconductor-plasma. A typical doped III-V semiconductor, n-InSb exposed to pulsed 10.6 µm CO_2 laser, has been numerically analysed to determine the relationship of threshold pump fields and gain coefficients for various values of externally supplied magnetostatic field and doping concentration. While acoustical phonon induced parametric instability occurs at a lower threshold than optical phonon induced parametric instability, we also discovered that the gain coefficients in acoustical phonon mode induced parametric amplification increase by a factor of 10 when compared to optical phonon induced parametric amplification. To lower thresholds and improve gain coefficients, a control parameter that applies a magnetostatic field externally can be used. These findings may be crucial for comprehending and enhancing the functionality of parametric amplifiers. The goal of this effort is to develop a low-cost parametric amplifier using the n-InSb-CO_2 system.

1. Introduction

It is considered a disturbance when phonons affect the velocity of electrons. Different forms of electron-phonon interactions are produced by these induced disturbances. The transport and optical characteristics of electrons in semiconductor media are significantly impacted by these interactions. Through their strain field, the low frequency acoustical phonon may modify the electron's energy. Deformation potentials can be used to describe these interactions. It is possible to think of optical phonons as creating internal strain, and optical phonon deformation potentials can be used to describe how they interact with electrons. In polar semiconductors, the charges connected with moving ions allow high/low frequency optical/acoustical phonons to produce electric fields. The Frohlich interaction in case of optical phonons and the piezoelectric phonon-electron interaction in case of acoustical phonons are two examples of how strongly the electric field may interact with electrons. Inter-valley electron-phonon interactions can cause electrons at band extremes close to or at boundary of the zone to scatter from one analogous valley to the other.

Different types of phonon-electron interactions, including piezoelectric interaction with acoustical phonons, the Frohlich interaction with the longitudinal optical (LO) phonons, the deformation potential interaction with both acoustical and optical phonons, are produced by these induced perturbations [1]. Through the piezoelectric effect, strain field creates electric field in non-centrosymmetric crystals. Certain directions can have piezoelectric activity from acoustic phonons. The electrical as well as optical characteristics of semiconductors have appreciably impacted via piezoelectric interaction of acoustical phonons with electron interactions to enhance device performance [2].

Because of the interesting application in photonic devices like ultra rapid optical switching and ultra dense memory, the phonon characteristics of bulk materials and reduced dimensional structures frequently catch the scientist's interest [3–8]. Quanta of atomic vibrations known as phonons are found in crystalline materials. In a crystalline material having N atoms in each primitive cell, there exist three acoustical phonons and $3N$-3 optical phonons. The optical phonons may be regarded as high frequency phonons, whereas the acoustical phonons are typically referred to as low frequency phonons. When attempting to comprehend the function of phonons in thermal and electrical characteristics of materials, acoustic phonons are crucial. They contribute significantly to the transport characteristics of technologically significant semiconductors along with optical phonons. In moderately doped semiconductors, they are the dominating heat carriers over the broad regime of temperature, from cryogenic to almost the melting point. A broad continuous spectrum regime, an almost linear dispersion curve, and the large carrier concentrations even at sufficiently lower temperature are characteristics of acoustic phonons in bulk materials [9]. It is well known that acoustical phonons impart greater role in scattering of carrier's and can even outweigh optical phonons in a low temperature regime [10]. Carriers regularly experience collisions with impurity atoms, crystal defects, and phonons (acoustic and optical), as they move through a device. The primary electron scattering mechanism for $A^{III}B^{V}$ semiconductors is scattering by acoustical and optical phonons, which has attracted a lot of attention owing to their possible use in regulating the carrier's relaxation to their band bottom, which is required for adequate lasing action, parametric amplification, and for transport and optical processes [11–13]. Because of their emerging uses in high speed tele-communication as well as photonic devices, the devices based on parametric processes in light withstanding materials are thought to have a unique position in nonlinear optical technology [14–16].

According to the literature that is currently available, there have apparently been no attempts where the growth (amplification) and threshold (excitation) properties of optical phonon-induced parametric amplification and acoustical phonon-induced parametric amplification in magnetised doped $A^{III}B^{V}$ semiconductors have been compared. The output characteristics of parametric devices based on said interactions will be improved by theoretical comprehension of this comparison. As a result, we examine these interactions in this study and evaluate how they affect the gain coefficient of parametrically amplified signal as well as threshold electric field needed to initiate the parametric amplification process. In light of the foregoing, we have analytically examined the parametric amplification characteristics brought on by pump-phonon interactions, specifically pump-acoustical phonon and pump-optical phonon interactions, using an n-InSb/CO_2 laser system at 77K temperature under applied transverse magnetic field.

2. Objectives

This work compares the effects of optical and acoustical phonons on parametric amplification in magnetised doped $A^{III}B^{V}$ semiconductors in order to determine the potential of the n-InSb/CO_2 laser system for production of inexpensive parametric amplifiers.

3. Theoretical formulations

This part ought to contain sufficient information to enable competent researchers to replicate the study in its entirety. New methods should have protocols, but established protocols can just be mentioned.

We take into account an external magnetostatic field $\vec{B}_0 = \hat{z}B_0$ and a homogeneous semiconductor medium with a spatially uniform ($|\vec{k}_0| = 0$) pump electric field $\vec{E}_0 = \hat{x}E_0 \exp(i\omega_0 t)$. To simplify the expression for quadratic susceptibility through induced polarisation, the coupled mode technique is used. Considered is the fluid model of semiconductor-plasmas: $kl << 1$, which limits the applicability of our analysis to the limit (k is the wave number and l is the carrier's mean free path). The fundamental equations as well as formulae for the lattice motion's equation for both acoustical phonon generated and optical phonon generated parametric amplification in $A^{III}B^{V}$ semiconductors are used from Refs. [17] and [18] in order to explore the comparison between the two interactions.

3.1. Threshold pump field and gain coefficient due to acoustical phonon induced parametric amplification

Since the unit cell lacks a centre of symmetry in the $A^{III}B^{V}$ type semiconductors having partially ionic bonds and unlike atoms, the scattering of carriers is caused by acoustical phonons as a result of piezoelectric scattering. An intense pump source creates the perturbation in an electron concentration (at frequency of acoustical field) in the process of acoustical phonon induced parametric amplification. This perturbation in electron concentration couples nonlinearly with pump field and generates an acoustical field. The pump field threshold needed to initiate parametric process and gain factor of parametrically amplified signal for pump fields significantly higher than the threshold field may be written as [17]:

$$(E_{0,th})_{AP} = \frac{m}{ek}\left(1-\frac{\omega_c^2}{\omega_0^2}\right)[(\Omega_{ps}^2+\nu^2\omega_s^2)(\Omega_{pa}^2+\nu^2\omega_a^2)]^{1/4} \quad (1)$$

and

$$(g_{para})_{AP} = -\frac{k_a k_s \omega_0^4 \omega_s \gamma^2 [\Gamma_a \omega_a (\omega_0^2-\omega_c^2)+\Omega_a^2 \nu\omega_0]}{\varepsilon_0 \eta c\rho(\Omega_a^4+4\Gamma_a^2\omega_a^2)[(\omega_0^2-\omega_c^2)^2+4\nu^2\omega_0^2]} \times\left(1+\frac{\delta_4}{\delta_3}\frac{\omega_p^2}{\omega_0\omega_s}\right), \quad (2)$$

where

$$\delta_3 = 1-\frac{(\Omega_{ps}^2 - i\nu\omega_s)(\Omega_{pa}^2+i\nu\omega_a)}{k_s^2\bar{E}^2}, \ \delta_4 = \left(1+\frac{(\beta/\gamma)\delta_1\delta_2}{E_0}\right),$$

$$\Omega_a^2 = \omega_a^2 - k_a^2 v_a^2, \ \Omega_{ps}^2 = \bar{\omega}_p^2-\omega_s^2, \ \Omega_{pa}^2 = \bar{\omega}_p^2 - \omega_a^2, \ \bar{E} = \frac{e}{m}(\vec{E}_{eff})$$

$$, \ \delta_1 = 1-\frac{\omega_c^2}{(\omega_0^2-\omega_c^2)}, \ \delta_2 = 1-\frac{\omega_c^2}{(\omega_s^2-\omega_c^2)}, \ \bar{\omega}_p = \frac{\nu\omega_p}{(\nu^2+\omega_c^2)^{1/2}},$$

$\omega_c = \frac{eB_0}{m}$ (electron-cyclotron frequency), and

$\omega_p = \left(\frac{n_0 e^2}{m\varepsilon}\right)^{1/2}$ (electron-plasma frequency).

3.2. Threshold pump field and gain coefficient due to optical phonon induced parametric amplification

Only low frequency acoustical phonons were considered in previous section when considering the phonon-electron scattering. These may be distinguished via sound velocity that is frequency independent. It is also necessary to consider "optical phonons" in $A^{III}B^{V}$ semiconductors having two or more atoms in each unit cell. Compound semiconductors have an ionic binding property that allows electromagnetic radiation to induce oscillation of atoms in optical phonons. A powerful pump source creates an electron concentration disturbance (at frequency of optical field) in the process of optical phonon induced parametric amplification. This electron concentration perturbation links nonlinearly with the pump field and drives an optical phonon field. The pump field threshold necessary to initiate parametric process and gain factor of parametrically amplified field for pump fields significantly higher than threshold field may be written as [18]:

$$(E_{0th})_{OP} = \frac{m}{ek}\frac{\Omega_{rs}\Omega_{rop}(\omega_0^2-\omega_c^2)}{[(\omega_0^2-\omega_{cx}^2)+\nu\omega_{cz}]} \quad (3)$$

and

$$(g_{para})_{OP} = \frac{\omega_s}{\eta c}[\chi_{eff}^{(2)}]_i, \quad (4)$$

where

$$\chi_{eff}^{(2)} = \frac{\varepsilon^2\omega_0^2 N\alpha_u}{2\varepsilon_0 M(\Omega_{rop}^2+i\Gamma\omega_{op})} + \frac{\varepsilon_\infty e^2 k_{op}(k_0-k_{op})}{\varepsilon_0 m^2\omega_0\omega_s(\Omega_{rs}^2+i\nu\omega_s)} \times\left[1-\frac{\varepsilon N}{2M(\Omega_{rop}^2+i\Gamma\omega_{op})}\left\{\frac{2q_s\alpha_u}{\varepsilon}-\alpha_u^2\left|(E_{eff})_x\right|^2\right\}\right].$$

$$\Omega_{rop}^2 = \bar{\omega}_r^2-\omega_{op}^2,\ \Omega_{rs}^2 = \bar{\omega}_r^2-\omega_s^2,\ \bar{\omega}_r^2 = \omega_r^2\left(\frac{\nu^2+\omega_{cx}^2}{\nu^2+\omega_c^2}\right),$$

in which

$$\omega_{cx,z}\left(=\frac{e}{m}B_{sx,z}\right),\ \omega_r^2 = \frac{\omega_p^2\omega_l^2}{\omega_t^2},$$

$$\omega_p = \left(\frac{n_e e^2}{m\varepsilon_0\varepsilon_L}\right)^{1/2} \text{ and } \frac{\omega_l}{\omega_t} = \left(\frac{\varepsilon_L}{\varepsilon_\infty}\right)^{1/2}.$$

ω_l is frequency of longitudinal optical phonon field. ε_L is lattice dielectric constant.

4. Results and discussion

This section discusses in-depth numerical analysis for potential amplification of the parametrically amplified wave based on the study performed in section 3. It is anticipated that an n-InSb crystal will be exposed to a pulsed 10.6 μm CO_2 laser at 77 K; the pertinent parameters are provided in Ref. [17]. The conflict between the threshold and amplification properties of the parametrically amplified waves caused by acoustical and optical phonons is the major topic of this research.

The ratio between the threshold pump field can be calculated using equations (1) and (3). One obtains

$$\frac{(E_{0th})_{AP}}{(E_{0th})_{OP}} = 1.67\times10^{-2} \text{ (at } B_0 = 14.2\text{ T and } n_0 = 10^{22}\text{ m}^{-3}\text{)}.$$

The gain coefficients' relationship to the material parameters can be calculated using equations (2) and (4). As a result, in both situations, given fixed input pump field greater than the threshold field, one obtains

$$\frac{(g_{para})_{AP}}{(g_{para})_{OP}} = 2\times10^2 \text{ (at } B_0 = 14.2\text{ T and } n_0 = 10^{22}\text{ m}^{-3}\text{)}.$$

Figures 1 - 4 show the numerical estimates of the external parameters (such as the carrier concentration, the magnetic field, etc.) that affect the threshold and amplification characteristics.

According to the externally applied magnetostatic field B_0 for the doping concentration $n_0 = 10^{22}$ m^{-3}, Figure 1 shows how the threshold electric field necessary to excite the acoustical phonon induced and optical phonon induced parametric amplification varies. The threshold fields $(E_{0th})_{AP}$ and $(E_{0th})_{OP}$ in this diagram stand for the acoustical phonon induced and optical phonon induced parametric amplification, respectively. It can be observed that smaller values of B_0 (< 2 T), both $(E_{0th})_{AP}$ and $(E_{0th})_{OP}$ are extremely high and the curves nearly coincide. With increasing magnetostatic field ($2\,\text{T} < B_0 < 13.5\,\text{T}$), both $(E_{0th})_{AP}$ and $(E_{0th})_{OP}$ decrease very slowly. With further increasing magnetostatic field, both $(E_{0th})_{AP}$ and $(E_{0th})_{OP}$ decrease sharply attaining a minimum value at $B_0 = 14.2$ T. Beyond this value of magnetostatic field, both $(E_{0th})_{AP}$ and $(E_{0th})_{OP}$ increase very rapidly, finally saturating at larger magnitudes of magnetic field ($B_0 \approx 16$ T). The dip at $B_0 = 14.2$ T occurs via resonance: $\omega_c^2 \sim \omega_0^2$ (between electron-cyclotron frequency and pump wave frequency). Moreover, for the regime of magnetic field plotted, we find $(E_{0th})_{AP} < (E_{0th})_{OP}$. As a result, we infer from this figure that the threshold electric field necessary to elicit the acoustical phonon-induced parametric amplification is significantly smaller than that required by the optical phonon-induced parametric amplification. Additionally, by putting the semiconductor crystal in a transverse magnetostatic field around resonance condition (electron-cyclotron frequency ~ pump wave frequency), it is possible to lower the threshold electric field needed to excite the parametric amplification caused by both the acoustical and optical phonons.

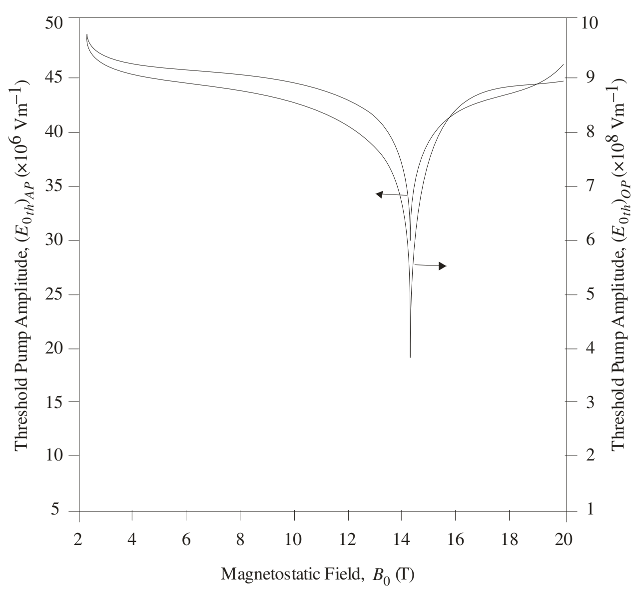

Figure 1. Variation of the threshold electric field w.r.t. magnetostatic field B_0 for doping concentration $n_0 = 10^{22}$ m^{-3}.

With respect to a large range of doping concentration n_0 (10^{19} m^{-3} to 10^{24} m^{-3}), Figure 2 illustrates the modification of the threshold electric field necessary to excite the acoustical phonon generated and optical phonon induced parametric amplification for externally applied magnetostatic field $B_0 = 14.2$ T. Here, $(E_{0th})_{AP}$ and $(E_{0th})_{OP}$ denote the threshold fields needed to elicit the parametric amplification caused by acoustical and optical phonons, respectively. With an increase in electron concentration, both $(E_{0th})_{AP}$ and $(E_{0th})_{OP}$ drop parabolically. Additionally, we discover $(E_{0th})_{AP} < (E_{0th})_{OP}$ for the regime of doping concentration plotted. From this figure, we infer that increased doping concentration is advantageous for reducing the threshold electric field needed to excite both the acoustical phonon induced parametric amplification and the optical phonon induced parametric amplification.

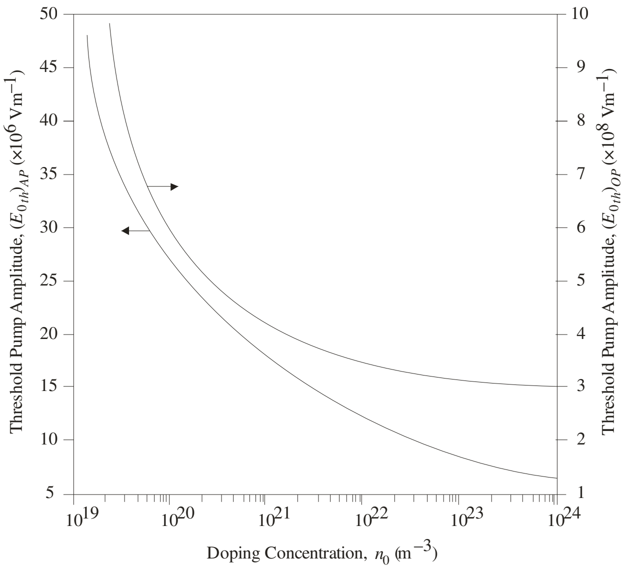

Figure 2. Variation of the threshold electric field required to incite the acoustical phonon induced and optical phonon induced parametric amplification w.r.t. wide range of doping concentration n_0 (10^{19} $\mathrm{m^{-3}}$ to 10^{24} $\mathrm{m^{-3}}$) for applied magnetostatic field B_0 = 14.2T.

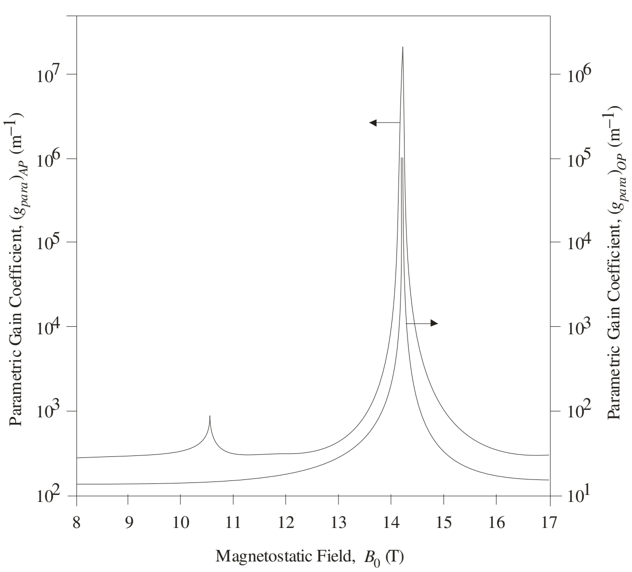

Figure 3. Nature of dependence of the gain coefficients due to acoustical phonon induced and optical phonon induced parametric amplification w.r.t. magnetostatic field B_0 for doping concentration n_0 = 10^{22} $\mathrm{m^{-3}}$ at $E_0 = 1.2\times10^8$ $\mathrm{Vm^{-1}}$.

For doping concentration $n_0 = 10^{22}\ \mathrm{m^{-3}}$ at $E_0 = 1.2\times10^8$ $\mathrm{Vm^{-1}}$, Figure 3 depicts the relationship between the gain coefficients resulting from parametric amplification caused by acoustical phonon induction and optical phonon induction with respect to an externally applied magnetostatic field. The gain coefficients resulting from the parametric amplification caused by the acoustical phonon induced and optical phonon induced are shown in this figure as $(g_{para})_{AP}$ and $(g_{para})_{OP}$, respectively. It is found that both $(g_{para})_{AP}$ and $(g_{para})_{OP}$ are nearly independent of magnetostatic field except at resonance conditions. $(g_{para})_{AP}$ shows sharp peaks around $B_0 = 10.6\ \mathrm{T}$ (due to resonance condition $\bar{\omega}_p^2 \sim \omega_s^2$; $(g_{para})_{AP} \propto \delta_4$ in confirmatory with Eq. (2)) and $B_0 = 14.2\ \mathrm{T}$ (due to resonance condition $\omega_c^2 \sim \omega_0^2$; $(g_{para})_{AP} \propto (\omega_0^2 - \omega_c^2)^{-2}$ in confirmatory with Eq. (2)). However, $(g_{para})_{OP}$ shows sharp peaks around $B_0 = 14.2\ \mathrm{T}$ (due to resonance condition $\omega_c^2 \sim \omega_0^2$; $(g_{para})_{AP} \propto (\omega_0^2 - \omega_c^2)^{-2}$ in confirmatory with Eq. (4)) only. A comparison between the two curves reveal that gain coefficient due to acoustical phonon induced parametric amplification is higher than due to optical phonon induced parametric amplification.

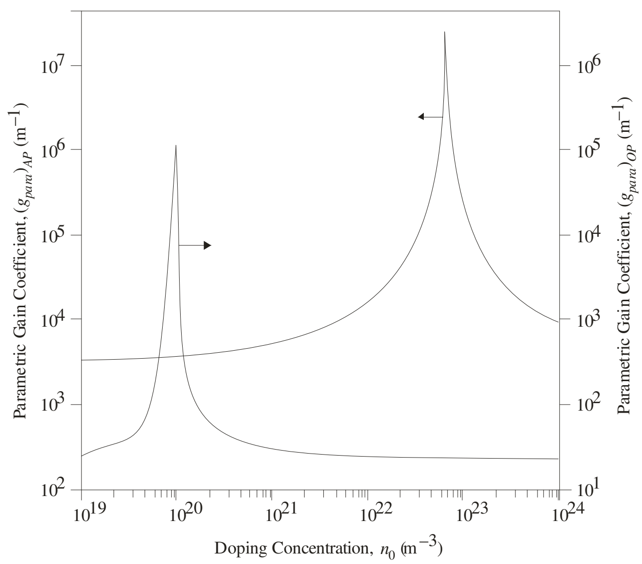

Figure 4. Variation of the gain coefficients due to acoustical phonon induced and optical phonon induced parametric amplification w.r.t. wide range of doping concentration n_0 (10^{19} $\mathrm{m^{-3}}$ to 10^{24} $\mathrm{m^{-3}}$) for externally applied magnetostatic field B_0 = 14.2 T at $E_0 = 1.2\times10^8$ $\mathrm{Vm^{-1}}$.

Figure 4 shows the variation of the gain coefficients due to acoustical phonon induced and optical phonon induced parametric amplification with respect to wide range of doping concentration n_0 ($10^{19}\ \mathrm{m^{-3}}$ to $10^{24}\ \mathrm{m^{-3}}$) for externally applied magnetostatic field $B_0 = 14.2\ \mathrm{T}$ at $E_0 = 1.2\times10^8\ \mathrm{Vm^{-1}}$. Here, $(g_{para})_{AP}$ and $(g_{para})_{OP}$ stand for the gain coefficients due to the acoustical phonon induced and optical phonon induced parametric amplification. It is found that $(g_{para})_{AP}$ shows sharp peak around $n_0 = 6\times10^{22}\ \mathrm{m^{-3}}$ while $(g_{para})_{OP}$ shows sharp peak around $n_0 = 10^{20}\ \mathrm{m^{-3}}$. A comparison between the two curves again confirms that gain coefficient due to acoustical phonon induced parametric amplification is higher than due to optical phonon induced parametric amplification. Hence, we conclude from this figure that the gain coefficients of acoustical phonon induced and optical phonon induced parametric amplification can be enhanced by suitably choosing the doping concentration. The results are well in agreement with the other theoretical observations made by S. Bhan et al. [19].

5. Conclusions

This work compares the threshold and gain coefficients of optical phonon-induced parametric amplification and acoustical phonon-induced parametric amplification. As opposed to optical phonon-induced parametric amplification, acoustical phonon-induced parametric amplification requires a substantially lower threshold electric field. Additionally, by putting the semiconductor crystal in a transverse magnetostatic field around resonance condition (electron-cyclotron frequency ~ pump wave frequency), it is possible to lower the threshold electric field needed to excite the parametric amplification caused by both the acoustical and optical phonons. A high doping concentration helps to reduce the threshold electric field needed to excite the parametric amplification caused by both optical and acoustic phonons. While the gain coefficient for optical phonon mode induced parametric amplification can only be increased due to resonance between electron cyclotron frequency and pump frequency, it can be enhanced at resonance between coupled cyclotron-plasmon frequency and Stokes frequency as well as between electron cyclotron frequency and pump frequency. Acoustical phonon-induced parametric amplification has a greater gain coefficient than optical phonon-induced parametric amplification, in addition. By carefully selecting the doping concentration, the gain coefficients of both optical and acoustical phonon-induced parametric amplification can be improved. This study challenges the usual notion of employing high power pulsed lasers and emphasises the significance of extensively doped magnetoactive III-V semiconductors as viable candidate materials for parametric amplification. As a result of this work, a low-cost parametric amplifier using the n-InSb-CO_2 system can be created.

References

[1] P.Y. Yu, M. Cardona, *Fundamentals of Semiconductors: Physics and Material Properties*, Springer, Berlin (1996).

[2] M. Dutta, M.A. Stroscio, K.W. Kim, Recent developments on electron-phonon interactions in structures for electronic and optoelectronic devices, *Int. J. High Speed Electron. Syst.* **9** (1998) 281-312.

[3] E.E. Vdovin, A. Levin, A. Patane, L. Eaves, P.C. Main, Yu N. Khanin, Yu V. Dubrovskii, M. Henini, G. Hill, Imaging the electron wave function in self assembled quantum dots, *Science* **290** (2000) 122-124.

[4] V.I. Klimov, A.A. Mikhailovsky, S. Xu, A. Malko, J.A. Hollingsworth, C.A. Leatherdale, H.J. Eisler, M.G. Bawendi, Optical gain and stimulated emission in nanocrystal quantum dots, *Science* **290** (2000) 314-317.

[5] A.J. Nozik, Spectroscopy and hot electron relaxation dynamics in semiconductor quantum wells and quantum dots, *Annu. Rev. Phys. Chem.* **52** (2001) 193-231.

[6] M. Bayer, P. Hawrylak, K. Hinzer, S. Fafard, M. Korkusinski, Z.R. Wasilewski, O. Stern, A. Forchel, Coupling and entangling of quantum states in quantum dot molecules, *Science* **291** (2001) 451-453.

[7] E. Ozbay, Plasmonics: Merging photonics and electronics at nanoscale dimensions, *Science* **311** (2006) 189-193.

[8] S. Sun, H. Kim, Z. Luo, G.S. Solomon, E. Waks, A single photon switch and transistor enabled by a solid state quantum memory, *Science* **361** (2018) 57-60.

[9] T. Kawamura, S.D. Sarma, Phonon-scattering-limited electron mobilities in $Al_xGa_{1-x}As$/GaAs heterojunctions, *Phys. Rev. B* **45** (1992) 3612-3627.

[10] S. Yu, K.W. Kim, A. Michael, A. Stroscio, G.J. Iafrate, A. Ballato, Electron-acoustic phonon scattering rates in rectangular quantum wires, *Phys. Rev. B* **50** (1994) 1733-1738.

[11] R. Fiederling, M. Keim, G. Reuscher, W. Ossau, G. Schmidt, A. Waag, L.W. Molenkamp, Injection and detection of a spin-polarized current in a light emitting diode, *Nature* **402** (1999) 787-790.

[12] P. Chang, A.G. Baca, N.Y. Li, X.M. Xie, H.Q. Hou, E. Armour, InGaP/InGaAsN/GaAs npn double-heterojunction bipolar transistor, *Appl. Phys. Lett.* **76** (2000) 2262-2264.

[13] A. Pandya, S. Shinde, P.K. Jha, Hot electron scattering rates via LO-phonon emission in two dimensional $GaAs_{1-x}N_x$, *Ind. J. Pure Appl. Phys*. **47** (2009) 523-526.

[14] N. Ishii, K. Kaneshima, T. Kania, S. Watanabe, J. Itatani, Generation of ultrashort intense optical pulses at 1.6 mm from a bismuth triborate-based optical parametric chirped pulse amplifier with carrier-envelope phase stabilization, *J. Opt*. **17** (2015) 094001.

[15] A. El-N. A. Mohamed, M.M.E. El-Halawany, A.N.Z. Rashed, M.M.A. Eid, Recent applications of optical parametric amplifiers in hybrid WDM/TDM local area optical networks, *Int. J. Comp. Sci. Inform. Security* **3** (2009) 1.

[16] M.E. Marhic, P.A. Andrekson, P. Petropoulos, S. Radic, C. Peucheret, M. Jazayerifar, Optical fiber parametric amplifiers in optical communication systems, *Laser Photon Rev*. **9** (2015) 50-74.

[17] M. Singh, M. Singh, Piezoelectric contributions to optical parametric amplification of acoustical phonons in magnetized doped III-V semiconductors, *Iran. J. Sci. Technol. Trans. Sci.* **45** (2021) 373-382.

[18] Sandeep, S. Dahiya, N. Singh, Parametric excitation of optical phonons in weakly-polar narrow band gap magnetized semiconductor plasmas, *Mod. Phys. Lett. B* **31** (2017) 1750294.

[19] S. Bhan, H.P. Singh, V. Kumar, Acoustical-phonon and polaron mode-induced optical parametric amplification in transversely magnetized III-V semiconductors, *Mod. Phys. Lett. B* **33** (2019) 1950271.